Efficient Preconditioning for the Discontinuous Galerkin Finite Element Method by Low-Order Elements

R. Hartmann [a], M. Lukáčová-Medviďová [b], F. Prill [a,b,*]

[a] *Institute of Aerodynamics and Flow Technology, German Aerospace Center (DLR), Braunschweig, Germany*

[b] *Institute of Numerical Simulation, Hamburg University of Technology, Hamburg, Germany*

Abstract

We derive and analyze a block diagonal preconditioner for the linear problems arising from a discontinuous Galerkin finite element discretization. The method can be applied to second-order self-adjoint elliptic boundary value problems and exploits the natural decomposition of the discrete function space into a global low-order subsystem and components of higher polynomial degree. Similar to results for the p-version of the conforming FEM, we prove for the interior penalty discontinuous Galerkin discretization that the condition number of the preconditioned system is uniformly bounded with respect to the mesh size of the triangulation. Numerical experiments demonstrate the performance of the method.

Key words: discontinuous Galerkin method, block diagonal preconditioning, static condensation, advection-diffusion equation
1991 MSC: 35J05, 35J25, 65N30, 65N35, 65F10, 65M22

1. Introduction

The so-called *hp*-finite element method (*hp*-FEM) achieves discrete numerical solutions for PDEs of high accuracy by refining the computational grid and/or increasing

* Corresponding author.
Email addresses: ralf.hartmann@dlr.de (R. Hartmann), lukacova@tu-harburg.de (M. Lukáčová-Medviďová), florian.prill@dlr.de (F. Prill).

the polynomial degree of the underlying finite element space. The partitioning of the domain is somewhat coarser than for the classical h-finite element method. Compared to the p-FEM, however, the hp-FEM uses polynomial shape functions of relatively low degree. Among the class of hp-FEM, the discontinuous Galerkin methods (dGFEM) for elliptic PDEs present a nonconforming specialty. The dGFEM use piecewise polynomial function spaces without continuity constraints on inter-element boundaries. In fact, the enforcement of the inter-element continuity as well as the imposition of boundary conditions is realized in a weak sense only.

Being originally introduced for hyperbolic problems [26], today a variety of methods for purely elliptic and convection-diffusion type problems can be discretized using discontinuous Galerkin methods; a list of existing discretization schemes has been analyzed in a unified framework in Arnold et al. [2]. The discontinuous approach enjoys great popularity for a wide range of PDEs, in particular due to its flexibility in mesh design (non-matching grids, hanging nodes, hp-refinement strategies) and a local stencil property amenable to parallelization [9, 20].

As a main drawback, however, the discontinuous Galerkin discretization leads to a relatively large number of degrees of freedom in comparison to other discretization methods. The corresponding linear systems are large, sparse, and rather ill-conditioned [7]. Thus, there is the need for optimal preconditioning forms to improve the overall efficiency and performance of the dGFEM.

By the term *optimal*, we mean the following: Given the bilinear form $B(u, v)$ that arises from the discretization of the problem, we need to construct a spectrally equivalent form $C(u, v)$, i.e. there exist constants m_1, $m_2 \in \mathbb{R}^+$ such that there holds for elements u_h of the discrete function space V_h

$$m_1 B(u_h, u_h) \leq C(u_h, u_h) \leq m_2 B(u_h, u_h). \tag{1}$$

Here, the inversion of the expression $C(u, v)$ should be easily obtainable. The overall objective would be an optimal iterative method where the rate of convergence towards the exact solution is independent of the number of unknowns. In view of the dGFEM and equation (1), this means that the constants m_1, m_2 are uniformly bounded with respect to the underlying partition and the local polynomial degree, or less strictly, growing only moderately with p.

In the context of the hp-FEM, a fundamental idea for the construction of optimal preconditioners is to derive a subsystem based on a suitable low-order discretization. The solution of this auxiliary problem is then used to develop an iterative solution method for the original system. The advantage of low-order preconditioning is twofold: For the linear systems arising from a discretization, for example with bilinear finite elements, efficient iterative methods, e.g. the h-multigrid method, are known and can be applied to the preconditioning form with low computational cost. Additionally, in terms of implementation, the low-order preconditioning is also a memory issue: The large, sparse stiffness matrix grows rapidly with the degree p of the shape functions. Neglecting boundary effects, and considering the matrix arising from a triangulation with n_t elements in a d-dimensional domain, and with s neighbouring relations in the operator stencil, the upper bound for the number of nonzero matrix entries is given by $nnz = n_t(s+1)(p+1)^{2d}$ provided a tensor product basis is used to span the local finite element spaces. A preconditioning system discretized based on bilinear elements is therefore smaller by a factor of $(2/(p+1))^{2d}$.

There exists a great variety of low-order preconditioning techniques in the literature: One possibility is to exploit the natural hierarchy of the discrete function spaces by successively decreasing the polynomial degree of the discretization while keeping the spatial partition unchanged. These historically early approaches, the so-called multi-p methods, can for example be found in [16, 17, 21, 27]. In a more general framework, related preconditioners are investigated in the field of multilevel domain decomposition methods [25, 31, 33]. Finally, we note that also algebraic multigrid techniques have been applied to the dGFEM, a description of two approaches together with applications can be found in [14, 19].

In this paper we describe another preconditioning approach that is related to the domain decomposition method: The iterative solver is constructed by substructuring, where the splitting of the finite element space is based on decomposing internal and external degrees of freedom on each element, which is possible for specific sets of basis functions like e.g. hierarchical basis functions. This is a well-known technique for the conforming p-FEM [3, 6, 22]. The goal of this paper is to generalize this technique for the dGFEM.

In particular, we introduce a dGFEM specific block preconditioning approach and prove that the condition number of the preconditioned system is uniformly bounded with respect to the mesh size of the triangulation. The estimate is also explicit with respect to the polynomial degree p and it is shown that the bound grows as $p^2(1+\log p)^2$. This result is less favorable than the corresponding one for the conforming finite element method. Therefore the preconditioning technique remains limited to dGFEM discretizations where the polynomial degree is chosen to be relatively small.

The paper is structured as follows: In Section 2 we briefly state the interior penalty discontinuous Galerkin discretization of a scalar elliptic model problem, along with some notation and the definition of the finite element spaces. Then, in Section 3, we formulate the diagonal preconditioners for the Schur complement arising from the dG discretization. Section 4 is devoted to the generalization of the convergence results from the p-FEM to the dGFEM non-conforming case. Then, we provide some numerical experiments in Section 5 demonstrating the feasiblity of the approach for purely diffusive problems and the case of moderate convection. Finally, we draw some conclusions in Section 6.

2. Model problem and discretization

In the following we state the model problem and its discretization based on the interior penalty method as well as introduce the polynomial basis employed.

2.1. *Model problem*

Let us consider the steady diffusion equation on a bounded domain $\Omega \subset \mathbb{R}^d$ with a sufficiently smooth boundary Γ:

$$\mathcal{L}u \equiv -\nabla \cdot (\boldsymbol{a} \nabla u) = -\sum_{i,j=1}^{d} \partial_i \left(a_{ij} \partial_j u\right) = f \quad \text{in } \Omega, \tag{2}$$

where $f \in L^2(\Omega)$ is a given function and the diffusivity tensor $\boldsymbol{a} = \{a_{ij}\}_{i,j\in\underline{d}} \in \mathbb{R}^{d\times d}$ is symmetric and positive definite. The coefficients a_{ij}, $(i,j) \in \underline{d} \times \underline{d}$, are assumed to be

bounded and piecewise constant. Here, we use the notation $\underline{n} := \{1, 2, \ldots, n\} \subset \mathbb{N}$ for $n \in \mathbb{N}$. Problem (2) is supplemented with Dirichlet boundary conditions, $u = g_{\mathrm{D}}$ on Γ, where $g_{\mathrm{D}} \in H^{1/2}(\Gamma)$.

2.2. *Meshes, trace operators and finite element spaces*

While concentrating on the two-dimensional case $d = 2$ in later sections, we will first formulate the discretization scheme for the general case. Let us assume that Ω can be subdivided into shape-regular meshes $\mathcal{T}_h$, consisting of convex open subsets (elements) $\kappa_j \neq \emptyset$, $j \in \underline{n_t}$, of characteristic size $h := \max_{j \in \underline{n_t}} (\operatorname{diam} \kappa_j)$:

$$\bar{\Omega} = \bigcup_{\kappa_j \in \mathcal{T}_h} \bar{\kappa}_j, \quad \kappa_i \cap \kappa_j = \emptyset \ \ \forall (i,j) \in \underline{n_t} \times \underline{n_t}, i \neq j, \quad n_t := \operatorname{card} \mathcal{T}_h.$$

Throughout this paper we confine ourselves to partitionings into quadrilateral elements, thus each element has $n_e := 2^d$ sides. We define the set $\mathcal{E}$ of all interior and boundary faces, i. e. the smallest $(d-1)$-dimensional intersection between neighbouring elements of the partition and between elements and the boundary Γ. Furthermore, we define the set of interior faces $\mathcal{E}_{\mathrm{int}} = \{e \in \mathcal{E} : e \subset \Omega\}$ and its union $\Gamma_{\mathrm{int}} := \{\boldsymbol{x} \in \Omega : \exists e \in \mathcal{E}_{\mathrm{int}} \text{ with } \boldsymbol{x} \in e\}$. As it was pointed out above, the dGFEM admits triangulations containing irregular vertices, also called hanging nodes, in a natural way.

We define $\mathcal{P}_p(\hat{\kappa})$ as the space of polynomials of degree at most $p \geq 0$ in d variables, restricted to the reference domain $\hat{\kappa} := I^d$, $I := [-1, 1]$. Furthermore, by $\mathcal{Q}_p(\hat{\kappa})$ we denote the tensor product space of one-dimensional polynomials of degree p, i. e. the space of functions on $\hat{\kappa}$ which are polynomials of degree less than or equal to p in each variable:

$$\mathcal{Q}_p(\hat{\kappa}) = \bigotimes_{i=1}^{d} \mathcal{P}_p(I).$$

Together with a unisolvent set of $n_{\hat{\kappa}} := \dim \mathcal{Q}_p(\hat{\kappa})$ linear independent functionals

$$\mathcal{F}_{\hat{\kappa}} = \{\mathcal{F}_1, \mathcal{F}_2, \ldots, \mathcal{F}_{n_{\hat{\kappa}}}\} \subset (\mathcal{Q}_p(\hat{\kappa}))^*$$

we obtain the reference finite element $(\hat{\kappa}, \mathcal{Q}_p(\hat{\kappa}), \mathcal{F}_{\hat{\kappa}})$, see Ciarlet [8]. We then construct the isoparametric finite element family on $\mathcal{T}_h$ with a sufficiently smooth bijective mapping $\sigma_\kappa : \hat{\kappa} \to \kappa$, $\sigma_\kappa \in [\mathcal{Q}_p(\hat{\kappa})]^d$ with a sufficiently smooth inverse σ_κ^{-1}, and get the local discrete function space

$$\mathcal{Q}_p(\kappa) := \{v \in L^2(\kappa) : v \circ \sigma_\kappa \in \mathcal{Q}_p(\hat{\kappa})\}, \quad \kappa \in \mathcal{T}_h,$$

and the global discrete function space

$$V_h^p := \{v \in L^2(\Omega) : v\big|_\kappa \in \mathcal{Q}_p(\kappa), \ \forall \kappa \in \mathcal{T}_h\}.$$

Some additional assumptions on the triangulation $\mathcal{T}_h$ and the mapping σ_κ are required to satisfy an equivalence between bilinear forms defined on the reference element $\hat{\kappa}$ and the element κ in real space: The deformation of the elements must be bounded, in the sense that there holds

$$\begin{aligned} \|\det(\nabla \sigma_\kappa)\|_{L^\infty(\hat{\kappa})} \leq Ch^2, \quad |\sigma_\kappa|_{1,\infty,\hat{\kappa}} := \max_{|\alpha|=1} (\operatorname{ess\,sup}_{\boldsymbol{x} \in \hat{\kappa}} |\partial^\alpha \sigma_\kappa|) \leq Ch, \\ \|\det(\nabla \sigma_\kappa^{-1})\|_{L^\infty(\kappa)} \leq Ch^{-2}, \quad |\sigma_\kappa^{-1}|_{1,\infty,\kappa} \leq Ch^{-1}. \end{aligned} \tag{3}$$

Given (3), the proof of equivalence between the bilinear forms is based simply on the chain rule, see [8] for more detail.

By $H^s(\mathcal{T}_h)$, $s \in \mathbb{R}^+$, we denote the broken Sobolev space, i. e. the space of functions on $\mathcal{T}_h$ whose restriction to an element $\kappa \in \mathcal{T}_h$ belong to $H^s(\kappa)$. For a function $v \in H^1(\mathcal{T}_h)$ we define v_κ^+, $\kappa \in \mathcal{T}_h$, to be the inner trace of v on $\partial\kappa$. The traces of functions in $H^1(\mathcal{T}_h)$ belong to the vector space

$$T(\Gamma \cup \Gamma_{\text{int}}) := \prod_{\kappa \in \mathcal{T}_h} L^2(\partial\kappa)$$

and are double-valued for $\boldsymbol{x} \in \Gamma_{\text{int}}$, while on the boundary, $\boldsymbol{x} \in \Gamma$, the value $v(\boldsymbol{x})$ is unambiguous [10]. For $\kappa \in \mathcal{T}_h$ with $\partial\kappa \setminus \Gamma \neq \emptyset$ there exists a neighbouring element $\kappa' \in \mathcal{T}_h$ that shares a common edge $e = \bar{\kappa} \cap \bar{\kappa}' \in \mathcal{E}_{\text{int}}$ with κ. The outer trace v_κ^- of v on e is defined as the inner trace v_κ^+ relative to the element κ'.

Furthermore, let us define the following jump and average operators. For $v \in H^1(\mathcal{T}_h)$ the jump of v on the edge $e = \bar{\kappa} \cap \bar{\kappa}' \in \mathcal{E}_{\text{int}}$ is given by

$$[\![v]\!]_e : T(\Gamma \cup \Gamma_{\text{int}}) \to L^2(\Gamma \cup \Gamma_{\text{int}}), \qquad [\![v]\!]_e = v_\kappa^+ \boldsymbol{n}_\kappa^+ + v_\kappa^- \boldsymbol{n}_\kappa^-,$$

where $\boldsymbol{n}_\kappa^+$ and $\boldsymbol{n}_\kappa^-$ denote the unit outward normal vectors to κ and κ', respectively. Additionally, the mean value of v on the edge e is defined as

$$\{v\}_e : T(\Gamma \cup \Gamma_{\text{int}}) \to L^2(\Gamma \cup \Gamma_{\text{int}}), \qquad \{v\}_e = \frac{1}{2}\left(v_\kappa^+ + v_\kappa^-\right).$$

For element boundaries $e \in \mathcal{E} \setminus \mathcal{E}_{\text{int}}$, that are part of the global domain boundary Γ, the boundary values are defined unambiguously. We set

$$[\![v]\!]_e = v^+ \boldsymbol{n}, \quad \{v\}_e = v^+ \text{ on } e.$$

For the sake of simplicity, the subscripts κ and e are omitted in the following.

2.3. *The discontinuous Galerkin discretization*

The interior penalty discontinuous Galerkin (IPdG) discretization [24] of the steady diffusion problem (2) is given in the following way: Find $u_h \in V_h^p$ such that

$$B^{\pm}(u_h, v_h) = \ell(v_h) \quad \forall v_h \in V_h^p, \tag{4}$$

where the bilinear form $B^{\pm}(\cdot,\cdot)$ is

$$\begin{aligned} B^{\pm}(u,v) := &\sum_{\kappa \in \mathcal{T}_h} \int_\kappa \boldsymbol{a}\nabla u \cdot \nabla v \, d\boldsymbol{x} + \int_{\Gamma_{\text{int}} \cup \Gamma} \theta\{\boldsymbol{a}\nabla v\} \cdot [\![u]\!] - \{\boldsymbol{a}\nabla u\} \cdot [\![v]\!] \, ds \\ &+ \int_{\Gamma_{\text{int}} \cup \Gamma} \sigma [\![u]\!] \cdot [\![v]\!] \, ds, \\ \ell(v) := &\int_\Gamma \theta((\boldsymbol{a}\nabla v) \cdot \boldsymbol{n}) g_{\text{D}} \, ds + \int_\Gamma \sigma g_{\text{D}} v \, ds, \quad \theta := \pm 1. \end{aligned} \tag{5}$$

Here, the sign factor θ distinguishes between the symmetric ($\theta = -1$) and the non-symmetric ($\theta = +1$) interior penalty discontinuous Galerkin discretization. The term $\sigma = \sigma(\boldsymbol{a}, h, p)$ denotes a stabilizing penalty parameter and is chosen for $e \in \mathcal{E} \cup \mathcal{E}_{\text{int}}$ as $\sigma\big|_e = \delta p^2 h^{-1} \|\sqrt{\boldsymbol{a}}\boldsymbol{n}_e\|^2_{L^\infty(e)}$, with a given factor $\delta > 0$. The weak formulation can be derived from a flux formulation related to the mixed-type FEM, see for example [2, 11].

2.4. *Hierarchical basis functions*

A discrete function $u_h \in V_h^p$ can be expanded into the sum

$$u_h(\boldsymbol{x}) = \sum_{i=1}^{n_h^p} u_i \phi_i(\boldsymbol{x}) = \sum_{\kappa \in \mathcal{T}_h} \sum_{i=1}^{n_\kappa} u_i^\kappa \phi_i^\kappa(\boldsymbol{x}),$$

where $n_h^p := \dim V_h^p$ and $n_\kappa := \dim \mathcal{Q}_p(\kappa)$ for $\kappa \in \mathcal{T}_h$. Here, $\boldsymbol{u} = (u_1, u_2, \ldots)^T \in \mathbb{R}^{n_h^p}$ and $\boldsymbol{u}^\kappa = (u_1^\kappa, u_2^\kappa, \ldots)^T \in \mathbb{R}^{n_\kappa}$, $\kappa \in \mathcal{T}_h$, include the coefficients of the discrete function on Ω and on a single element κ, respectively. Furthermore, the set $\mathcal{B}_p = \{\phi_i^\kappa\}_{i \in \underline{n_\kappa}}$, $\kappa \in \mathcal{T}_h$, consists of the local basis functions of $\mathcal{Q}_p(\kappa)$. Then, the global basis $\{\phi_j\}_{j \in \underline{n_h^p}} \equiv \left\{\phi_{\pi(\kappa,i)}\right\}_{\kappa \in \mathcal{T}_h, i \in \underline{n_\kappa}}$ of the discrete function space V_h^p is constructed based on $\mathcal{B}_p$ where $\pi : \mathcal{T}_h \times \underline{n_\kappa} \to \underline{n_h^p}$ denotes the global numbering of the degrees of freedom. Using this notation the discrete problem (4) can be translated into an algebraic system $\underline{\boldsymbol{A}}\boldsymbol{u} = \boldsymbol{f}$ where the global system matrix $\underline{\boldsymbol{A}} \in \mathbb{R}^{n_h^p \times n_h^p}$ is assembled by summing up the element stiffness matrices $\underline{\boldsymbol{A}}^{(\kappa)} \in \mathbb{R}^{n_\kappa \times n_\kappa}$.

In the p-FEM context a common choice for the basis $\mathcal{B}_p$ for $\mathcal{Q}_p(\kappa)$ is the hierarchical tensor product basis formed by the Babuška-Szabó polynomials [18, 29, 32]. On the two-dimensional reference element $\hat{\kappa}$ they are defined as

$$\begin{aligned}
\hat{\mathcal{B}}_{p,\text{modal}} &:= \left\{\hat{L}_{ij} : 0 \le i,j \le p\right\} \subset \mathcal{Q}_p([-1,1]^2),\\
\hat{L}_0(x) &= \frac{1-x}{2},\ \hat{L}_1(x) = \frac{1+x}{2},\\
\hat{L}_k(x) &= \frac{1}{\|L_{k-1}\|_{L^2(-1,1)}} \int_{-1}^{x} L_{k-1}(\xi)\ d\xi,\ 2 \le k \le p,\\
\hat{L}_{ij}(x,y) &= \hat{L}_i(x)\hat{L}_j(y),\ 0 \le i,j \le p,
\end{aligned} \tag{6}$$

where $L_k(x)$ are the Legendre polynomials. The basis $\hat{\mathcal{B}}_{p,\text{modal}}$ of the local discrete function space $\mathcal{Q}_p(\kappa)$ is termed hierarchical since it satisfies $\hat{\mathcal{B}}_{p-1,\text{modal}} \subset \hat{\mathcal{B}}_{p,\text{modal}}$, i. e. the set of basis functions of V_h^{p-1} is a subset of that of V_h^p.

An important feature of the tensor product basis $\hat{\mathcal{B}}_{p,\text{modal}}$ is the fact that the set of shape functions can be decomposed into a set of external (boundary) modes $\mathcal{N}_\mathcal{W}$ and the set of internal shape functions $\mathcal{N}_\mathcal{I}$.

In the two-dimensional case, where the notions for sides and edges coincide, the external-internal decomposition is given by

$$\mathcal{Q}_p(\hat{\kappa}) = \mathcal{W}^p(\hat{\kappa}) \oplus \mathcal{I}^p(\hat{\kappa}), \tag{7}$$

where the vector space of external functions is formed as

$$\mathcal{W}^p(\hat{\kappa}) := \mathcal{P}_1(\hat{I}_1) \otimes \mathcal{P}_p(\hat{I}_2) \cup \mathcal{P}_p(\hat{I}_1) \otimes \mathcal{P}_1(\hat{I}_2),$$

spanned by the external vertex shape functions $\mathcal{N}_\mathcal{V} := \left\{\hat{L}_{ij}(x,y) : 0 \le i,j \le 1\right\}$, and the edge shape functions $\mathcal{N}_\mathcal{E} = \left\{\hat{L}_{i,j}, \hat{L}_{j,i} : i = 0,1; 2 \le j \le p\right\}$. Here, we have $\hat{I}_i := \left\{\xi \in \mathbb{R}^d : \xi_i \in I, \xi_j = 0, i \ne j\right\}$. The vector space spanned by the internal shape functions

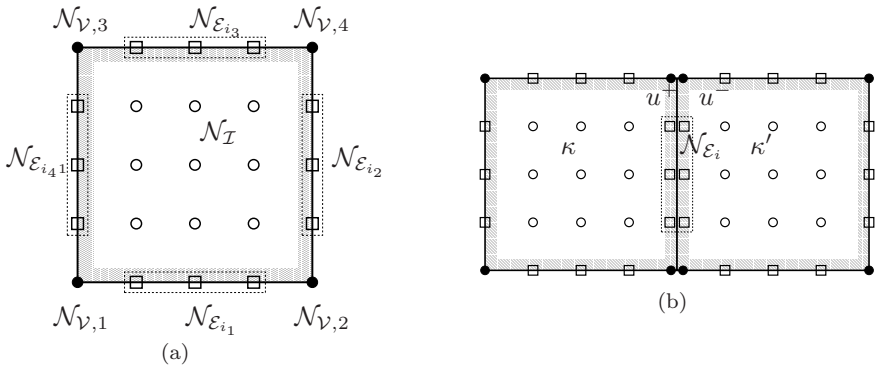

Figure 1. External-internal decomposition on the quadrilateral reference element, $p = 4$. The different symbols mark the locations of the degrees of freedom (DoFs). The right picture illustrates the six DoFs corresponding to a single edge $\mathcal{E}_i$.

can be constructed using a bubble function $b_{\hat{\kappa}}(x, y) := 16\hat{L}_{0,0}\hat{L}_{1,1} = (1 - x^2)(1 - y^2)$, and is given by

$$\mathcal{I}^p(\hat{\kappa}) := \{b_{\hat{\kappa}} v : v \in \mathcal{Q}_{p-2}(\hat{\kappa})\}\,.$$

After a suitable ordering of the degrees of freedom the elemental stiffness matrix has the block structure

$$\underline{A}^{(\kappa)} = \begin{pmatrix} \underline{A}^{(\kappa)}_{\mathcal{I}\mathcal{I}} & \underline{A}^{(\kappa)}_{\mathcal{I}\mathcal{W}} \\ \underline{A}^{(\kappa)}_{\mathcal{W}\mathcal{I}} & \underline{A}^{(\kappa)}_{\mathcal{W}\mathcal{W}} \end{pmatrix}, \quad \underline{A}^{(\kappa)}_{\mathcal{W}\mathcal{W}} = \begin{pmatrix} \underline{A}^{(\kappa)}_{\mathcal{E}\mathcal{E}} & \underline{A}^{(\kappa)}_{\mathcal{E}\mathcal{V}} \\ \underline{A}^{(\kappa)}_{\mathcal{V}\mathcal{E}} & \underline{A}^{(\kappa)}_{\mathcal{V}\mathcal{V}} \end{pmatrix}, \tag{8}$$

where the subscripts $\mathcal{I}$ and $\mathcal{W}$ correspond to the set of internal and external shape functions, respectively. The subscripts $\mathcal{V}$, $\mathcal{E}$ distinguish between the vertex (bilinear) and edge components of the elemental basis (in three dimensions, the elemental matrix (8) includes also blocks corresponding to the element faces). Finally, the submatrices are of the sizes $\underline{A}^{(\kappa)}_{\mathcal{A}_1\mathcal{A}_2} \in \mathbb{R}^{n_{\mathcal{A}_1} \times n_{\mathcal{A}_2}}$, $n_{\mathcal{A}_i} := \mathrm{card}\,\mathcal{N}_{\mathcal{A}_i}$, for $\mathcal{A}_i \in \{\mathcal{I}, \mathcal{W}, \mathcal{E}, \mathcal{V}\}$. We note that $n_{\mathcal{W}} = n_{\mathcal{E}} + n_{\mathcal{V}}$ and $n_\kappa = n_{\mathcal{I}} + n_{\mathcal{W}}$.

For the symmetric interior penalty dG discretization both the matrices $\underline{A}$ and the matrix $\underline{C}_A^{-1}$ corresponding to the preconditioning form are $n_h^p \times n_h^p$ symmetric positive definite matrices. The preconditioned conjugate gradient method (PCG) used to solve the system of linear equations $\underline{A}\boldsymbol{u} = \boldsymbol{f}$ requires in each step the evaluation of the matrix-vector product $\underline{A}\boldsymbol{x}$ for a given vector $\boldsymbol{x}$ and the solution of the auxiliary problem $\underline{C}_A\boldsymbol{x} = \boldsymbol{r}$ for a given vector $\boldsymbol{r}$. This method satisfies the error bound [33]

$$\|\underline{A}^{-1}\boldsymbol{f} - \boldsymbol{x}^k\|_{\underline{A}} \le 2\eta_{\underline{A}}^k \|\underline{A}^{-1}\boldsymbol{f} - \boldsymbol{x}^0\|_{\underline{A}},$$

where the convergence factor is given by

$$\eta_{\underline{A}} = \frac{\sqrt{\kappa_2(\underline{C}_A^{-1}\underline{A})} - 1}{\sqrt{\kappa_2(\underline{C}_A^{-1}\underline{A})} + 1}. \tag{9}$$

The PCG method allows an approximation of the condition number $\kappa_2(\underline{C}_A^{-1}\underline{A})$ due to its close relationship to the symmetric Lanczos process [28, 34].

Remark 1 *In the examples given in Section 5 we will also investigate the linear systems arising from nonsymmetric forms such as the nonsymmetric interior penalty dG discretization of the diffusion equation and the dG discretization of convection-diffusion problems. We then resort to the GMRES method [28], which is a Krylov subspace method suitable also for nonsymmetric, indefinite matrices. In this case, however, theoretical bounds for the convergence of the method are less satisfying and will not be considered here.*

3. Schur complement preconditioner

We now describe a generalization of the p-FEM preconditioner of Babuška et al. [3] for the dG finite element method.

3.1. *Schur complement of the stiffness matrix*

In a first step we eliminate the unknowns corresponding to the internal shape functions. This concept is widely used in the p-FEM context, where it is denoted by *partial orthogonalization* or *static condensation*. As was pointed out by Sherwin et al. [30], the elimination procedure can also be applied to the dGFEM when using a C^0-type expansion basis like the one defined in (6).

Formally, for the dG discretization there exist no edge and vertex shape functions in the strict sense, since each degree of freedom is associated with a single element only. Instead, continuity between the elements is enforced in a weak sense by introducing the inter-element jump terms. However, in the case of an external-internal decomposition (7), the inter-element jump terms act only on the external shape functions in $\mathcal{W}^p(\hat{\kappa})$.

After the static condensation procedure the linear system is given by

$$\begin{pmatrix} \underline{A}_{\mathcal{I}\mathcal{I}} & \underline{A}_{\mathcal{I}\mathcal{W}} \\ 0 & \underline{S} \end{pmatrix} \begin{pmatrix} \boldsymbol{u}_{\mathcal{I}} \\ \boldsymbol{u}_{\mathcal{W}} \end{pmatrix} \equiv \sum_{\kappa\in\mathcal{T}_h} \begin{pmatrix} \underline{A}^{(\kappa)}_{\mathcal{I}\mathcal{I}} & \underline{A}^{(\kappa)}_{\mathcal{I}\mathcal{W}} \\ 0 & \underline{S}^{(\kappa)} \end{pmatrix} \begin{pmatrix} \boldsymbol{u}^{(\kappa)}_{\mathcal{I}} \\ \boldsymbol{u}^{(\kappa)}_{\mathcal{W}} \end{pmatrix} = \sum_{\kappa\in\mathcal{T}_h} \begin{pmatrix} \boldsymbol{f}^{(\kappa)}_{\mathcal{I}} \\ \boldsymbol{f}^{(\kappa)}_{\mathcal{W}} - \underline{A}^{(\kappa)}_{\mathcal{W}\mathcal{I}}(\underline{A}^{(\kappa)}_{\mathcal{I}\mathcal{I}})^{-1}\boldsymbol{f}^{(\kappa)}_{\mathcal{I}} \end{pmatrix} \equiv \begin{pmatrix} \boldsymbol{f}_{\mathcal{I}} \\ \tilde{\boldsymbol{f}}_{\mathcal{W}} \end{pmatrix}, \tag{10}$$

with the global Schur complement operator

$$\underline{S} := \underline{A}_{\mathcal{W}\mathcal{W}} - \underline{A}_{\mathcal{W}\mathcal{I}}\underline{A}^{-1}_{\mathcal{I}\mathcal{I}}\underline{A}_{\mathcal{I}\mathcal{W}}, \quad \underline{S} \in \mathbb{R}^{N_{\mathcal{W}}\times N_{\mathcal{W}}}, \quad N_{\mathcal{W}} := n_t n_{\mathcal{W}}. \tag{11}$$

To describe the elemental parts $\underline{S}^{(\kappa)} \in \mathbb{R}^{N_{\mathcal{W}}\times N_{\mathcal{W}}}$ we introduce some additional notation: The discrete formulation of the bilinear form (5), restricted to a particular element $\kappa \in \mathcal{T}_h$, can be split into a sum of local terms $\underline{A}^{\kappa,\kappa}$ which consist of the volume integral term in (5) together with contributions of the face integrals, and face terms $\underline{A}^{\kappa_1,\kappa_2}$ which originate from the surface integral terms over an edge $e = \kappa_1 \cap \kappa_2$. The row of the global stiffness matrix $\underline{A}$ corresponding to the element κ is given by

$$(\underline{A}\boldsymbol{u})_\kappa = \underline{A}^{\kappa,\kappa}\boldsymbol{u}^\kappa + \sum_{\bar{\kappa}\in\mathcal{J}(\kappa)} \underline{A}^{\kappa,\bar{\kappa}}\boldsymbol{u}^{\bar{\kappa}}, \tag{12}$$

where $\mathcal{J}(\kappa)$ denotes the set of element neighbours defined by

$$\mathcal{J}(\kappa) := \{\bar{\kappa} \in \mathcal{T}_h \ : \ \partial\bar{\kappa} \cap \partial\kappa \in \mathcal{E}_{\text{int}}\}, \quad \kappa \in \mathcal{T}_h.$$

The blocks $\underline{A}^{\kappa,\kappa}$ and $\underline{A}^{\kappa,\bar{\kappa}}$, $\kappa \in \mathcal{T}_h$, $\bar{\kappa} \in \mathcal{J}(\kappa)$, in (12) are assembled by collecting all terms including test functions ϕ_i^κ on the element κ, and are given by

$$\begin{aligned}
(\underline{A}^{\kappa,\kappa})_{ij} =& \int_\kappa \boldsymbol{a}\nabla_h\phi_i^\kappa \cdot \nabla_h\phi_j^\kappa \, d\boldsymbol{x} \\
&+ \frac{1}{2}\int_{\partial\kappa} \theta\left(\boldsymbol{a}\nabla_h\phi_i^\kappa\right)\cdot\boldsymbol{n}\,\phi_j^\kappa - \left(\boldsymbol{a}\nabla_h\phi_j^\kappa\right)\cdot\boldsymbol{n}\,\phi_i^\kappa \, ds + \int_{\partial\kappa}\sigma\phi_i^\kappa\phi_j^\kappa \, ds, \\
\left(\underline{A}^{\kappa,\bar{\kappa}}\right)_{ij} =& \frac{1}{2}\int_{\partial\kappa\cap\partial\bar{\kappa}} \left[\theta\left(\boldsymbol{a}\nabla_h\phi_i^\kappa\right)\cdot\boldsymbol{n}\,\phi_j^{\bar{\kappa}} - \left(\boldsymbol{a}\nabla_h\phi_j^{\bar{\kappa}}\right)\cdot\boldsymbol{n}\,\phi_i^\kappa\right] \, ds, \quad i,j \in \underline{n_\kappa}.
\end{aligned} \tag{13}$$

Using this notation, $\underline{S}^{(\kappa)}$ can be represented as follows

$$\underline{S}^{(\kappa)} = \left(\underline{S}^{(\kappa)}_{\bar{\kappa},\bar{\bar{\kappa}}}\right)_{\bar{\kappa},\bar{\bar{\kappa}}\in\mathcal{J}(\kappa)\cup\{\kappa\}} \equiv \left(\left[\delta_{\kappa\bar{\kappa}}\underline{A}^{\bar{\kappa},\bar{\bar{\kappa}}}_{\mathcal{W}\mathcal{W}} - \left(\underline{A}^{\bar{\kappa},\kappa}_{\mathcal{W}\mathcal{I}}\right)\left(\underline{A}^{\kappa,\kappa}_{\mathcal{I}\mathcal{I}}\right)^{-1}\left(\underline{A}^{\kappa,\bar{\bar{\kappa}}}_{\mathcal{I}\mathcal{W}}\right)\right]\right)_{\bar{\kappa},\bar{\bar{\kappa}}\in\mathcal{J}(\kappa)\cup\{\kappa\}}. \tag{14}$$

The Kronecker symbol δ_{ij} in (14) avoids summing each element term $\underline{A}^{\kappa,\kappa'}_{\mathcal{W}\mathcal{W}}$ twice: In the usual implementation of the dGFEM stiffness matrix assembly, each face $e \in \mathcal{E}_{\text{int}}$ is considered only once. This is not the case for the element-wise assembly of the Schur matrix $\underline{S}$, where all edges of all elements must be traversed. In the actual implementation this can be avoided using an intermediate storage.

The submatrix $\underline{A}_{\mathcal{I}\mathcal{I}}$ is block diagonal. The inner subproblems $\underline{A}^{(\kappa)}_{\mathcal{I}\mathcal{I}}\boldsymbol{v} = \boldsymbol{w}$ are equivalent to the solution of a homogeneous Dirichlet problem, discretized with continuous FE and restricted to a single element κ of the triangulation. Therefore the solution of the second block row in equation (10) decomposes into a number of local subproblems which can be inverted at elemental level.

The formulation (14) leads to another observation: The Schur matrix has a less sparse nonzero structure than the original stiffness matrix, in the sense that the matrix stencil comprises also neighbour elements of second degree. Its direct assembly therefore should be avoided. In fact, it is not needed for Krylov iterative methods.

The reduced algebraic system is now given by $\underline{S}\boldsymbol{u}_{\mathcal{W}} = \tilde{\boldsymbol{f}}_{\mathcal{W}}$, where the matrix $\underline{S}$ has block structure:

$$\underline{S} \equiv \begin{pmatrix} \underline{S}_{\mathcal{E}\mathcal{E}} & \underline{S}_{\mathcal{E}\mathcal{V}} \\ \underline{S}_{\mathcal{V}\mathcal{E}} & \underline{S}_{\mathcal{V}\mathcal{V}} \end{pmatrix}. \tag{15}$$

For a symmetric form, like e.g. $B^-(u,v)$ in (5), this matrix is also symmetric.

In view of the original stiffness matrix $\underline{A}$, we obtain the decomposition

$$\underline{A} = \begin{pmatrix} \underline{I} & \underline{0} \\ \underline{A}_{\mathcal{W}\mathcal{I}}\underline{A}^{-1}_{\mathcal{I}\mathcal{I}} & \underline{I} \end{pmatrix} \begin{pmatrix} \underline{A}_{\mathcal{I}\mathcal{I}} & \underline{0} \\ \underline{0} & \underline{S} \end{pmatrix} \begin{pmatrix} \underline{I} & \underline{A}^{-1}_{\mathcal{I}\mathcal{I}}\underline{A}_{\mathcal{I}\mathcal{W}} \\ \underline{0} & \underline{I} \end{pmatrix},$$

which can be verified simply by substituting (11).

In the case that effective preconditioning matrices $\underline{B}_S^{-1}$ for the Schur complement (15), and for the inner subproblems $\underline{A}_{\mathcal{I}\mathcal{I}}$, $\underline{B}_{\mathcal{I}\mathcal{I}}^{-1}$, are available, we get a preconditioner for $\underline{A}$ of the form

$$\underline{C}_A^{-1} = \begin{pmatrix} \underline{I} & -\underline{B}_{\mathcal{I}\mathcal{I}}^{-1}\underline{A}_{\mathcal{I}\mathcal{W}} \\ \underline{0} & \underline{I} \end{pmatrix} \begin{pmatrix} \underline{B}_{\mathcal{I}\mathcal{I}}^{-1} & \underline{0} \\ \underline{0} & \underline{B}_S^{-1} \end{pmatrix} \begin{pmatrix} \underline{I} & \underline{0} \\ -\underline{A}_{\mathcal{W}\mathcal{I}}\underline{B}_{\mathcal{I}\mathcal{I}}^{-1} & \underline{I} \end{pmatrix}.$$

In fact, inserting the inverse matrices $\underline{S}^{-1}$ and $\underline{A}_{\mathcal{I}\mathcal{I}}^{-1}$, the expression would result into the expensive but exact preconditioner $\underline{C}_A^{-1} = \underline{A}^{-1}$. In the next section we describe a more realistic and efficient choice.

Remark 2 *The process of static condensation is equivalent to a change of the elemental basis. The local edge polynomials are replaced by discrete harmonic shape functions, i. e.* $\tilde{\mathcal{B}}_p = \mathcal{N}_{\mathcal{V}} \cup \tilde{\mathcal{N}}_{\mathcal{E}}$*, where*

$$\text{span } \tilde{\mathcal{N}}_{\mathcal{E}} = \{v \in \mathcal{N}_{\mathcal{E}} \oplus \mathcal{N}_{\mathcal{I}} : B(v, w) = 0 \ \forall w \in \mathcal{N}_{\mathcal{I}}\}.$$

This point of view is particularly useful when establishing energy estimates for a convergence proof. Note that the support of these basis functions is no longer restricted to single elements of the triangulation.

3.2. *Diagonal and edge block preconditioning*

This iterative substructuring method is among the earliest low-order preconditioners for the p-FEM. To apply its idea to the discontinuous discretization we introduce the canonical restriction operators $\underline{R}_{\mathcal{E}_i} \in \mathbb{R}^{n_{\mathcal{E}_i} \times n_h^p}$, $\underline{R}_{\mathcal{V}} \in \mathbb{R}^{n_{\mathcal{V}} \times n_h^p}$ along with the prolongations $\underline{R}_{\mathcal{E}_i}^T$, $\underline{R}_{\mathcal{V}}^T$, corresponding to the vector spaces spanned by the side and vertex shape functions of the discretization. Here, by $\mathcal{E}_i$ we denote the linear space spanned by those polynomials in V_h^p with non-vanishing support on a single edge $e_i \in \mathcal{E}_{\text{int}}$. An example set of edge degrees of freedom is illustrated in Figure 1(b).

Now we define the preconditioner $\underline{B}_S^{-1}$ by means of an additive Schwarz-type method

$$\underline{B}_S^{-1} = \sum_{\mathcal{E}_i \in \mathcal{E}} \underline{R}_{\mathcal{E}_i}^T (\underline{S}_{\mathcal{E}_i\mathcal{E}_i})^{-1} \underline{R}_{\mathcal{E}_i} + \underline{R}_{\mathcal{V}}^T \underline{S}_{\mathcal{V}\mathcal{V}}^{-1} \underline{R}_{\mathcal{V}}, \tag{16}$$

i. e. the preconditioning step consists of the solution of a global system $\underline{S}_{\mathcal{V}\mathcal{V}}^{-1}$, that arises from the discretization with bilinear elements, together with a number of independent local subproblems.

Translated into a matrix-vector notation, the procedure is the following: We obtain the preconditioning matrix by simply eliminating the off-diagonal blocks in (15) that connect the unknowns from the vertex and edge spaces. We further drop the subblocks representing the coupling between all pairs of edges $\mathcal{E}_i$, $1 \le i \le n_e$, which leads to the block-diagonal structure

$$\underline{B}_S := \begin{pmatrix} \underline{S}'_{\mathcal{E}\mathcal{E}} & \underline{0} \\ \underline{0} & \underline{S}_{\mathcal{V}\mathcal{V}} \end{pmatrix}, \quad \underline{S}'_{\mathcal{E}\mathcal{E}} = \text{blockdiag}\,(\underline{S}_{\mathcal{E}_i\mathcal{E}_i}). \tag{17}$$

Babuška et al. [3] have shown for the two-dimensional Laplace equation discretized by the conforming p-FEM, that the following condition number estimate holds:

$$\kappa_2(\underline{B}_S^{-1}\underline{S}) \leq C(1+\log p)^2. \tag{18}$$

Remark 3 *In three dimensions the degrees of freedom associated with the element faces have to be considered as well. The direct approach* (16) *does not lead to a result comparable to equation* (18)*. Special wire basket preconditioners have to be constructed instead, see for example Pavarino and Widlund [23].*

It is possible to simplify the preconditioner described above in the following way: The subproblems $(\underline{S}_{\mathcal{E}_i\mathcal{E}_i})^{-1}$ can be replaced by single diagonal entries of the Schur matrix,

$$\tilde{\underline{S}}_{\mathcal{E}\mathcal{E}}^{-1} = \operatorname{diag}(\underline{S}_{\mathcal{E}_i\mathcal{E}_i})^{-1}. \tag{19}$$

This reduces greatly the computational effort. However, for the p-FEM it has been shown by Casarin [6], that this particular variant leads to a slight deterioration of the convergence properties, in fact the condition number grows faster than polylogarithmically with p. In the numerical experiments for the discontinuous case in Section 5 we investigate also the reduced version of the preconditioner $\tilde{\underline{B}}_S^{-1}$.

4. Theoretical bounds

In this section we establish theoretical bounds for the factors m_1, m_2 in the preconditioning inequality (1). This happens along the lines of [3, 29], but we have to take special care of the interior face and boundary terms arising in the dG discretization (5).

We focus on the Poisson problem, i. e. $\boldsymbol{a} \equiv \mathbb{1}$. First, we consider the decomposition of the global bilinear form into elemental parts

$$B^{\pm}(u,v) = \sum_{\kappa\in\mathcal{T}_h} B_\kappa^{\pm}(u,v).$$

The choice of $B_\kappa^{\pm}(\cdot,\cdot)$ is not unambiguous. Here, instead of the form (13) which naturally arises by collecting all terms in equation (1) containing a test function local to κ, we use an edge-centred formulation similar to [19]:

$$\begin{aligned} B_\kappa^{\pm}(u,v) := &\int_\kappa \nabla u\cdot\nabla v \; d\boldsymbol{x} + \frac{1}{2}\sum_{s=1}^{n_e}\int_{e_s} \sigma(v^+\boldsymbol{n}^+ + v^-\boldsymbol{n}^-)\cdot(u^+\boldsymbol{n}^+ + u^-\boldsymbol{n}^-)\; ds \\ &+ \frac{1}{2}\sum_{s=1}^{n_e}\int_{e_s} \left[\theta\nabla v^+\cdot(u^+\boldsymbol{n}^+ + u^-\boldsymbol{n}^-) - (v^+\boldsymbol{n}^+ + v^-\boldsymbol{n}^-)\cdot\nabla u^+\right]\; ds, \end{aligned} \tag{20}$$

where n_e denotes the number of element sides. The specific feature of this formulation is the fact that derivatives occur on the cell κ only, while neighbouring cells contribute through their values on the cell boundary $\partial\kappa$. Furthermore, we note that constant functions lie within the kernel of $B_\kappa^{\pm}(u,u)$, in contrast to the bilinear form given in (13). It is noteworthy to mention that an alternative formulation like in (20) is possible for only some of the dG methods collected in e.g. [2], including the interior penalty variants. We point out that the proof given below does not rely on a uniform polynomial degree.

To avoid abundant notation, we identify the restriction matrices $\underline{R}_{\mathcal{V}}$, $\underline{R}_{\mathcal{E}_i}$, $\underline{R}_{\mathcal{I}}$ with their function space counterparts. For a given function $u_h \in V_h^p$, we define $u_{\mathcal{V}} = \underline{R}_{\mathcal{V}} u_h$,

$u_{\mathcal{E},i} = \underline{R}_{\mathcal{E}_i} u_h$, $i \in \underline{n_e}$, and $u_{\mathcal{I}} = \underline{R}_{\mathcal{I}} u_h$. Note, that $u_h\big|_\kappa = u_{\mathcal{V}}\big|_\kappa + \sum_{i\in\underline{n_e}} u_{\mathcal{E},i}\big|_\kappa + u_{\mathcal{I}}\big|_\kappa$. Then the block diagonal preconditioner $C = \operatorname{diag}(\underline{B}_{\mathcal{I}\mathcal{I}}, \underline{B}_S)$ is given by

$$C^{\pm}(u,v) = \sum_{\kappa\in\mathcal{T}_h} C^{\pm}_\kappa(u,v), \quad C^{\pm}_\kappa(u,v) := B^{\pm}_\kappa(u_{\mathcal{V}}, u_{\mathcal{V}}) + \sum_{i=1}^{n_e} B^{\pm}_\kappa(u_{\mathcal{E},i}, u_{\mathcal{E},i}) + B^{\pm}_\kappa(u_{\mathcal{I}}, u_{\mathcal{I}}). \tag{21}$$

Under the assumption of a regular subdivision $\mathcal{T}_h$ of Ω into shape-regular elements (possibly containing hanging nodes), and a sufficiently smooth and bounded bilinear mapping σ_κ to the reference cell $\hat{\kappa}$, see equation (3), it is sufficient to focus on the elemental preconditioning inequality

$$\hat{m}_1 B^{\pm}_{\hat{\kappa}}(u_h, u_h) \le C^{\pm}_{\hat{\kappa}}(u_h, u_h) \le \hat{m}_2 B^{\pm}_{\hat{\kappa}}(u_h, u_h), \tag{22}$$

for all discrete functions $u_h \in V_h$. Note, that in the following the superscript $\pm$ will be omitted, if possible.

Below, we state sufficient requirements for the preconditioning inequality. The statement can be proven by summing over the individual parts of u_h.

Theorem 1 *Assume that for the bilinear form $B_{\hat{\kappa}}(\cdot,\cdot)$ the following assumptions hold.*

(i) For any two vectors $a, b \in V_h^p$, the form B_κ satisfies a general triangle inequality

$$B_{\hat{\kappa}}(a+b, a+b) \le C\left(B_{\hat{\kappa}}(a,a) + B_{\hat{\kappa}}(b,b)\right) \tag{23}$$

with $C > 0$ independent of the mesh size h and the polynomial degree p.

(ii) For a given function $u_h \in V_h^p$, the vertex, side, and interior components satisfy energy bounds

$$\begin{aligned} B_{\hat{\kappa}}(u_{\mathcal{V}}, u_{\mathcal{V}}) &\le b_1 B_{\hat{\kappa}}(u_h, u_h), \\ B_{\hat{\kappa}}(u_{\mathcal{E},i}, u_{\mathcal{E},i}) &\le b_2 B_{\hat{\kappa}}(u_h, u_h), \ i = 1, \dots, n_e, \\ B_{\hat{\kappa}}(u_{\mathcal{I}}, u_{\mathcal{I}}) &\le b_3 B_{\hat{\kappa}}(u_h, u_h), \end{aligned} \tag{24}$$

with factors $b_i > 0$, $i \in \{1,2,3\}$.

Then the elemental preconditioning inequality (22)*, and thus the global property* (1)*, is fulfilled with bounds*

$$\frac{\hat{m}_2}{\hat{m}_1} \le C\left(b_1 + n_e b_2 + b_3\right).$$

Proof: The result follows immediately from the substitution of equations (23), (24) into the definition of the preconditioning form (16). □

The first inequality (23) can be deduced from the proof of boundedness and coercivity of $B_\kappa(\cdot,\cdot)$ with respect to the norm $\|\!|\cdot|\!\|^2_{dG}$ on the space $\tilde{V}_h^p := \left\{v \in V_h^p \ : \ \int_\Gamma v = 0\right\}$ defined as

$$\|\!|u|\!\|^2_{dG} := |u|^2_{H^1(\kappa)} + \sum_{s=1}^{n_e} \int_{e_s} \frac{\sigma}{2} [\![u]\!]^2 \, ds + \sum_{s=1}^{n_e} \int_{e_s} \sigma^{-1} (\nabla u \cdot \boldsymbol{n})^2 \, ds. \tag{25}$$

Except for the third term, this expression is a localized version of the one defined in [24], and it is the natural norm for proving boundedness of the bilinear form $B_\kappa(\cdot,\cdot)$. Note that the first two summands in equation (25) are identical to the expression $B^+_\kappa(u,u)$, which implies that the inequality (23) is trivially fulfilled for the nonsymmetric IPdG variant. The following lemma is particularly useful for the symmetric IPdG version.

Lemma 2

(i) The form $B_\kappa(\cdot,\cdot)$ is bounded with respect to the norm $\|\!|\cdot|\!\|_{dG}$, i. e. there exists $C_B > 0$ independent of h, p, such that

$$|B_\kappa(u_h, v_h)| \leq C_B \|\!|u_h|\!\|_{dG} \|\!|v_h|\!\|_{dG} \quad \forall u_h, v_h \in V_h^p. \tag{26a}$$

(ii) The form $B_\kappa(\cdot,\cdot)$ is coercive on $\tilde{V}_h^p$ with respect to the norm $\|\!|\cdot|\!\|_{dG}$, i. e. there exists $\delta_0 > 0$, such that for $\delta = \sigma h p^{-2} > \delta_0$ there exists $\alpha > 0$ independent of h, p, with

$$B_\kappa(u_h, u_h) \geq \alpha \|\!|u_h|\!\|_{dG}^2 \quad \forall u_h \in \tilde{V}_h^p. \tag{26b}$$

Proof: The proof is a slight modification of the Theorems 3.3, 3.5 in [24]. □

Before presenting the main result of this section, we collect some discrete inverse inequalities for later use. They can be found, for example, in the monograph by Schwab [29]. Here and in the following by C we denote a generic constant.

Lemma 3 *For a given polynomial function $v \in \mathcal{Q}_p(\hat{\kappa})$ on the reference element $\hat{\kappa}$ and one of its sides $e_i \subset \partial\hat{\kappa}$, $i = 1, \ldots, n_e$, we have*

$$\|v\|_{L^\infty(e_i)} \leq Cp\|v\|_{L^2(e_i)}, \tag{27a}$$

$$\|v\|_{L^\infty(\hat{\kappa})} \leq C(1+\log p)^{\frac{1}{2}} \|v\|_{H^1(\hat{\kappa})}, \tag{27b}$$

$$\|v\|_{L^2(e_i)} \leq Cp\|v\|_{L^2(\hat{\kappa})}. \tag{27c}$$

In the following we now state the main theoretical result.

Theorem 4 *For the block diagonal preconditioner* (21) *applied to the statically condensed linear system, both the assumptions* (23) *and* (24) *in Theorem 1 are satisfied with*

$$b_i \leq Cp^2(1+\log p)^2, \quad i \in \{1,2,3\}. \tag{28}$$

Remark 4 *The estimate* (28) *exhibits a strong p-dependency of the block diagonal preconditioner, in contrast to the conforming case [3] where, with the exception of the serendipity FE space, we have an estimate of the form* (18)*. The p-dependence is due to the presence of the additional terms introduced by the inter-element boundaries, and limits its use for p-adaptive variants of the discontinuous Galerkin method. However, the independence from the spatial refinement h is still satisfied.*

Proof:[Thm. 4] We begin by considering the inequality (23). For nonconstant functions $a, b \in \tilde{V}_h^p$ we use the bilinearity of $B_{\hat{\kappa}}$ and Lemma 2 and obtain

$$\begin{aligned} B_{\hat{\kappa}}(a+b, a+b) &\leq B_{\hat{\kappa}}(a,a) + B_\kappa(b,b) + C_B \|\!|a|\!\|_{dG} \|\!|b|\!\|_{dG} \\ &\leq B_{\hat{\kappa}}(a,a) + B_{\hat{\kappa}}(b,b) + \frac{1}{2} C \left(\|\!|a|\!\|_{dG}^2 + \|\!|b|\!\|_{dG}^2 \right) \\ &\leq C \left(B_{\hat{\kappa}}(a,a) + B_{\hat{\kappa}}(b,b) \right). \end{aligned}$$

Now it remains to show (24).

Let $u_h \in \tilde{V}_h^p$ be a given nonconstant function. The elemental bilinear form (20) remains unchanged when adding a constant $\lambda \in \mathbb{R}$ to the function u_h. Therefore, we may choose λ such that on the element $\hat{\kappa}$ a local Poincaré inequality

$$\|u_h\|_{H^1(\hat{\kappa})} \leq C|u_h|_{H^1(\hat{\kappa})} \tag{29}$$

is satisfied. This cannot be fulfilled on the neighbouring cells at the same time. However, we make extensive use of (29) when estimating the cell integral term in (25) similar to [3]. Beginning with a bilinear function $u_{\mathcal{V}}$ we have, due to (26a) and $u_{\mathcal{V}} \in V_h^p$,

$$B_{\hat{\kappa}}(u_{\mathcal{V}}, u_{\mathcal{V}}) = |u_{\mathcal{V}}|^2_{H^1(\hat{\kappa})} + \|\frac{\sigma}{2}[\![u_{\mathcal{V}}]\!]\|^2_{L^2(\partial\hat{\kappa})} + \frac{1}{2}\sum_{s=1}^{n_e}\int_{e_s} \theta\nabla u_{\mathcal{V}} \cdot [\![u_{\mathcal{V}}]\!]_{e_s} - [\![u_{\mathcal{V}}]\!]_{e_s}\nabla u_{\mathcal{V}}\ ds$$
$$\leq C|\!|\!|u_{\mathcal{V}}|\!|\!|^2_{dG} = C|u_{\mathcal{V}}|^2_{H^1(\hat{\kappa})} + C\sum_{s=1}^{n_e}\int_{e_s}\frac{\sigma}{2}[\![u_{\mathcal{V}}]\!]^2_{e_s}\ ds + C\sum_{s=1}^{n_e}\int_{e_s}\sigma^{-1}(\nabla u_{\mathcal{V}}\cdot\boldsymbol{n})^2\ ds.$$

For the cell term, we can resort to the proof for the conforming p-FEM [3, 29]. Thus, applying the discrete Sobolev inequality (27b), we have

$$|u_{\mathcal{V}}|^2_{H^1(\hat{\kappa})} \leq C\|u_{\mathcal{V}}\|^2_{L^\infty(\hat{\kappa})} \leq C(1+\log p)|u_h|^2_{H^1(\hat{\kappa})}.$$

Now only the boundary integrals of the dG formulation require special treatment. For the penalization term using the discrete inverse inequalities (27a) we get

$$\begin{aligned}\|[\![u_{\mathcal{V}}]\!]\|^2_{L^2(e_s)} &\leq C\|[\![u_{\mathcal{V}}]\!]\|^2_{L^\infty(e_s)} \leq C\|[\![u_h]\!]\|^2_{L^\infty(e_s)} \\ &\leq Cp^2\|[\![u_h]\!]\|^2_{L^2(e_s)}, \quad s \in \underline{n_e}. \end{aligned} \tag{30}$$

The remaining boundary terms are treated as follows.

$$\begin{aligned}\int_{e_s}(\nabla u_{\mathcal{V}}\cdot\boldsymbol{n})^2\ ds &= \|\nabla u_{\mathcal{V}}\cdot\boldsymbol{n}\|^2_{L^2(e_s)} \leq Cp^2\|\nabla u_{\mathcal{V}}\|^2_{L^2(\hat{\kappa})} \leq Cp^2\|\nabla u_{\mathcal{V}}\|^2_{L^\infty(\hat{\kappa})} \\ &\leq Cp^2\|u_{\mathcal{V}}\|^2_{L^\infty(\hat{\kappa})} \leq Cp^2(1+\log p)|u_h|^2_{H^1(\hat{\kappa})}. \end{aligned} \tag{31}$$

All results obtained so far occur in the elemental norm $|\!|\!|\cdot|\!|\!|_{dG}$. Thus, the discrete Schwarz inequality can be applied, and with the coercivity of the bilinear form we get the result

$$B_{\hat{\kappa}}(u_{\mathcal{V}}, u_{\mathcal{V}}) \leq Cp^2(1+\log p)B_{\hat{\kappa}}(u_h, u_h),$$

i. e. $b_1 := p^2(1+\log p)$ in (24).

For the second energy bound, we consider the difference function $\hat{u}_h := u_h - u_{\mathcal{V}}$, which vanishes on the element vertices. Babuška et al. [3] utilize a polynomial trace lifting $\tilde{u}_{\mathcal{E},i}$ to arrive at

$$|u_{\mathcal{E},i}|^2_{H^1(\hat{\kappa})} \leq C|\tilde{u}_{\mathcal{E},i}|^2_{H^1(\hat{\kappa})} \leq C(1+\log p)^2|u_h|^2_{H^1(\hat{\kappa})},$$

under the assumption that the side functions are discretely harmonic, cf. Remark 3. This estimate can be used for the dGFEM as well. Here, we construct $\tilde{u}_{\mathcal{E},i}$ from the trace lifting and the side functions $\hat{u}^{\bar{\kappa}}_{\mathcal{E},i}$, $\bar{\kappa} \in \mathcal{J}(\kappa)$. Since the interior part $u_{\mathcal{I}}$ vanishes on the element boundary $\partial\hat{\kappa}$, there holds

$$\|[\![\hat{u}_h]\!]\|_{L^2(e_s)} = \|[\![u_{\mathcal{E},i}]\!]\|_{L^2(e_s)}, \quad s = 1, \ldots, n_e. \tag{32}$$

Furthermore, we have for $i = 1, \ldots, n_e$,

$$\sum_{s=1}^{n_e}\int_{e_s}(\nabla\hat{u}_{\mathcal{E},i}\cdot\boldsymbol{n})^2\ ds \leq Cp^2\|(\nabla\hat{u}_{\mathcal{E},i}\cdot\boldsymbol{n})\|^2_{L^2(\hat{\kappa})} \leq Cp^2\|\nabla\hat{u}_{\mathcal{E},i}\|^2_{L^2(\hat{\kappa})} = Cp^2|\hat{u}_{\mathcal{E},i}|^2_{H^1(\hat{\kappa})}.$$

Thus, we obtain for the side components the result

$$B_{\hat{\kappa}}(\hat{u}_{\mathcal{E},i}, \hat{u}_{\mathcal{E},i}) \leq Cp^2(1+\log p)^2 B_{\hat{\kappa}}(\hat{u}_h, \hat{u}_h), \quad i \in \underline{n_e}.$$

Finally, the last energy estimate in (24) follows from the bound for the side components and the triangle inequality (23) applied to $u_{\mathcal{I}} = \hat{u}_h - \sum_{i=1}^{n_e}\hat{u}_{\mathcal{E},i}$. □

Remark 5 *Due to the special bilinear form* (20)*, the proof of Theorem 4 is similar to the conforming case [3]. The upper bounds for the inter-element boundary terms, however, introduce a strong p-dependency, since they are established via the L^∞-norm, see the equations* (30) - (32)*. This dG-specific drawback renders the block Jacobi preconditioner useful only for discretizations with bounded polynomial degree.*

5. Numerical examples

In the following we present numerical results for two test examples in order to demonstrate the feasibility of the proposed approach. All computations have been performed using the DG solver `PADGE` [13] based on the `deal.II` library [4, 5].

Problem 1 *Consider the Poisson equation on the unit square domain $\Omega = [0,1]^2$ with homogeneous Dirichlet boundary conditions, and constant data $\boldsymbol{f} \equiv 1$.*

Problem 2 *Consider the linear advection-diffusion problem*

$$\mathcal{L}_{ad}\, u \equiv -\nabla \cdot (\boldsymbol{a} \nabla u) + \nabla \cdot (\boldsymbol{b} u) = 0 \tag{33}$$

on the unit square. For the advection direction we choose the vector field $\boldsymbol{b}(x_1, x_2) := [-x_2, x_1]^T$, the diffusivity tensor is set to $\boldsymbol{a} := \epsilon \mathbb{1}$, $\epsilon > 0$, cf. Figure 8(b). Here, the interesting limit case will be $\epsilon \ll 1$. The description of the boundary conditions as well as the dGFEM formulation of the hyperbolic part is given below.

The tests will be performed on three different partitionings of the domain. The first family of tesselations $\mathcal{T}_{h_i}^1$, $i = 0, 1, 2, \ldots$, is constructed by successively dividing each element $\kappa \in \mathcal{T}_{h_{i-1}}^1$ into four quadrilaterals of equal size to obtain $\mathcal{T}_{h_i}^1$, i. e. we have $h_0 = 1, h_1 = \frac{1}{2}, \ldots$, and discretization sizes $n_{t,0} = 1, n_{t,1} = 4, \ldots, n_{t,6} = 4096$. Besides, we consider also a second tesselation of Ω, $\mathcal{T}_h^2$, with 448 elements containing hanging nodes originating from a local refinement process in the vicinity of the origin. The third test partitioning $\mathcal{T}_h^3$ is a so-called *B-type* grid [12] obtained by distributing half of the $(N+1)^2$ grid points equidistantly in a region $[\tau, 1] \times [0, 1]$, and locating the remaining nodes at $x_i := -\gamma\epsilon \ln(1 - 2(1-\epsilon)\frac{i}{N})$, $y_i := \frac{i}{N}$, $i = 0, 1, \ldots, \frac{N}{2}$, with given constants ϵ, γ. The transition point for the boundary layer region thus lies at $\tau := \gamma\epsilon |\ln \epsilon|$. We choose here $\gamma = 10$, $\epsilon = 10^{-3}$, $N = 50$. The maximum aspect ratio is therefore given by $\max_{i \in \underline{N}} N^{-1}(x_i - x_{i-1})^{-1} \approx 49.043$ for $\epsilon = 10^{-3}$. Note that we use this triangulation in spite of the fact that anisotropic partitionings violate the assumption (3). Examples of all three test partitionings are shown in Figure 2.

In Example 1, the stabilizing parameter σ is taken as $\sigma(p,h) = 2.5\frac{p^2}{h}$ for all grids. Here the cell diameter h is computed element-wise. We choose $\sigma = 2.5\epsilon\frac{p^2}{h}$ in Example 2. The linear problems for $p = 1$ are solved directly using the LU decomposition for small triangulation sizes. The subproblems for the larger test cases are solved inexactly using an inner GMRES iteration with block SSOR preconditioning. The global Schur complement matrix is not explicitly assembled, since it is less sparse than the original stiffness matrix.

5.1. *Scalar elliptic model problem*

First, we compare the estimated spectral condition number of the original stiffness matrix with that of the condensed system. For this test, we solve the Poisson problem

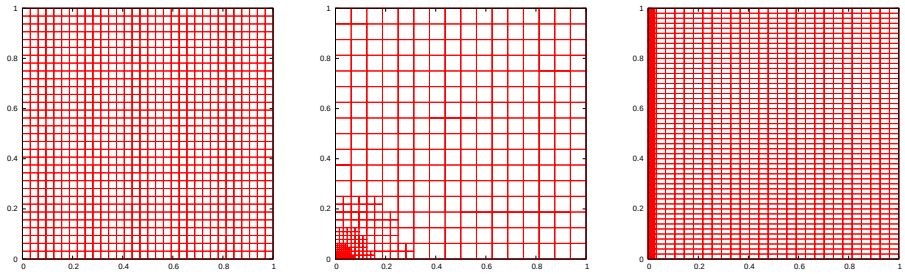

(a) Grid 1, $\mathcal{T}^1_{h_5}$ (b) Grid 2, $\mathcal{T}^2_h$ (c) Grid 3, $\mathcal{T}^3_h$

Figure 2. Partitionings of $\Omega = [0,1]^2$ for the numerical examples in Section 5.

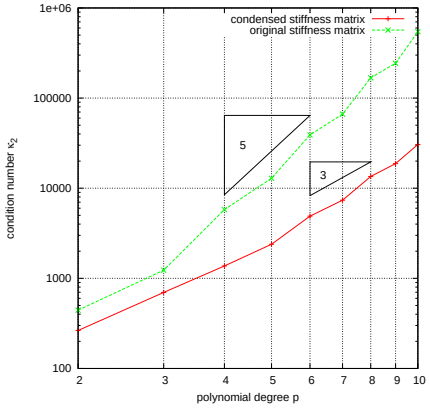

(a) Condition numbers.

p	n_h^p	$\dim \mathcal{W}^p(\Omega)$	$\dim \mathcal{I}^p(\Omega)$
2	9216	8192	1024
3	16384	12288	4096
4	25600	16384	9216
5	36864	20480	16384
6	50176	24576	25600

(b) Subspace dimensions for the triangulation $\mathcal{T}^1_{h_5}$.

Figure 3. Comparison of the (approximated) condition numbers (left) and subspace dimensions for the original stiffness matrix and the statically condensed system, discretized with different polynomial degrees.

on a uniform triangulation $\mathcal{T}^1_{h_4}$. Similar to the statement in [30] for the Bassi-Rebay and Local dGFEM, we observe a beneficial effect of the static condensation procedure. In Figure 3(a) the spectral condition number of the condensed stiffness matrix exhibits a cubic growth with respect to the polynomial degree p, while the original system seems to grow like p^5.

Next, we apply the preconditioners constructed in Section 3 to the Poisson model problem. Here it is of particular interest, whether the preconditioned system is independent of the characteristic mesh size h. To verify this, the linear systems corresponding to a nested hierarchy of partitionings $\mathcal{T}^1_{h_3}, \ldots, \mathcal{T}^1_{h_6}$ are solved while keeping the polynomial degree $p = 3$ constant. First the unpreconditioned conjugate gradient algorithm is applied to the symmetric positive systems. As it is illustrated in Figure 4(a), the problem exhibits strong dependence on the grid size, which can be seen by the fast growing number of linear iterations needed to converge the linear residual $\|\underline{S}^{-1}\tilde{\boldsymbol{f}}_{\mathcal{W}} - \boldsymbol{u}^k_{\mathcal{W}}\|_2$ to a given accuracy. In contrast, for the PCG iterations that are preconditioned using the block diagonal method (17) or the simplified diagonal edge version (19), no h-dependency is

	$\mathcal{T}^1_{h_1}$	$\mathcal{T}^1_{h_2}$	$\mathcal{T}^1_{h_3}$	$\mathcal{T}^1_{h_4}$	$\mathcal{T}^1_{h_5}$	$\mathcal{T}^1_{h_6}$
CG	116.449	364.383	698.234	2496.45	9783.96	38952.0
PCG, block diagonal $\underline{B}_S^{-1}$	23.2378	24.0041	24.1668	24.2069	24.2678	24.3506
PCG, diagonal $\tilde{\underline{B}}_S^{-1}$	55.5739	64.7979	67.8921	68.6512	69.1475	69.3022

	$\mathcal{T}^2_{h_1}$	$\mathcal{T}^2_{h_2}$	$\mathcal{T}^2_{h_3}$
CG	3105.19	12158.3	48345.0
PCG, block diagonal $\underline{B}_S^{-1}$	94.86	94.98	105.10
PCG, diagonal $\tilde{\underline{B}}_S^{-1}$	105.88	105.87	111.90

Table 1
Approximated condition numbers $\kappa_2(\underline{B}_S^{-1}\underline{S})$ for the (preconditioned) Schur complement system. Hierarchy of triangulations, Problem 1, $p = 3$.

	$\mathcal{T}^1_{h_1}$	$\mathcal{T}^1_{h_2}$	$\mathcal{T}^1_{h_3}$	$\mathcal{T}^1_{h_4}$	$\mathcal{T}^1_{h_5}$	$\mathcal{T}^1_{h_6}$
unpreconditioned	12	66	136	216	352	> 500
block diagonal preconditioner	24	32	33	32	31	33
diagonal preconditioner	34	59	69	70	70	67

Table 2
Iteration counts of the GMRES method for the solution of the Schur complement system for the non-symmetric IPdG discretization $B^+(u, v)$ of Problem 1.

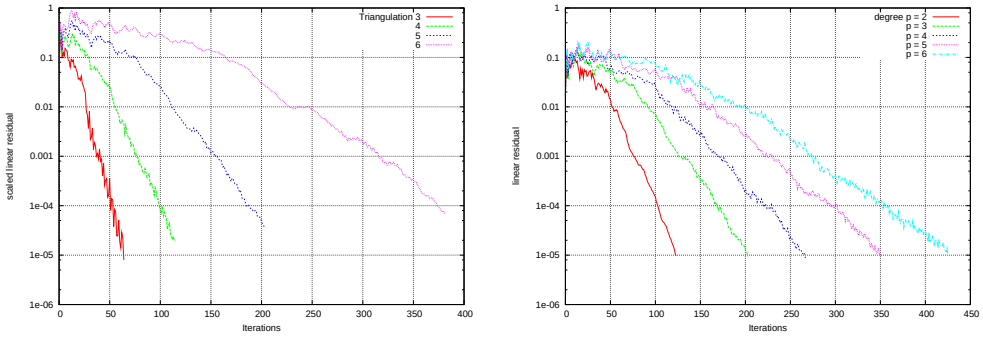

(a) Hierarchy of triangulations, $p = 3$.

(b) Varying polynomial degree p on $\mathcal{T}^1_{h_5}$.

Figure 4. Solution process of CG method for the Schur complement system arising from Problem 1. No preconditioning, iterations vs. residual norm.

observed, see Figures 6(a) and 5(a), respectively. Note that for all iteration plots, the graphs are scaled to coincide at the beginning of the iterations.

As stated in equation (9) the convergence rate of the conjugate gradient method is directly related to the condition number of the matrix product $\underline{C}_A^{-1}\underline{A}$. In fact, all observations made above find their counterpart in the condition number estimates obtained during the CG iteration, see the first part of Table 1. The approximate condition number κ_2 of the unpreconditioned system increases rapidly for smaller mesh sizes h, as it is shown in the first row of Table 1. On the other hand, listed in the second row, the block diagonal preconditioner yields an asymptotically bounded condition number for the uniformly refined tesselations $\mathcal{T}^1_h$. For the case of the reduced, diagonal preconditioning matrix, there seems to be a moderate h-dependence, however, as the condition number estimates stated in the third row slightly deteriorate.

Furthermore, we test the preconditioners for the problem discretized on the uniform partitioning $\mathcal{T}^1_{h_5}$ with 1024 elements with respect to its p-dependency. Results are less favorable here: Both, the unpreconditioned system as well as the diagonal edge preconditioner require a growing number of linear iterations with increasing polynomial degree $p = 2, \ldots, 6$, cf. Figures 4(b) and 5(b), while the block diagonal preconditioner does not give a clear picture for the small test case considered, see Figure 6(b). Nevertheless, to illustrate the advantage of the static condensation procedure in terms of memory efficiency, Table 3(b) provides a list of the subspace dimensions for varying polynomial degree. In particular it shows the savings by elimination of the bubble function components.

The behavior of the block diagonal preconditioner with respect to the polynomial degree p is in agreement with the theoretical bound obtained in Theorem 4. Figure 7 shows the development of the condition number, which seems to grow like $Cp^2(1+\log p)$. This is slightly better than the analytical result (28).

We now address the scalability of the proposed preconditioners applied to the nonsymmetric interior penalty discretization. Table 2 shows the number of steps for the GMRES method required to converge the solution to an absolute residual norm tolerance of 10^{-10}. Similar to the symmetric case, the block diagonal preconditioner seems to scale optimally with respect to the grid size.

To conclude this section, we consider the second family of test partitions, $\mathcal{T}^2_h$, containing

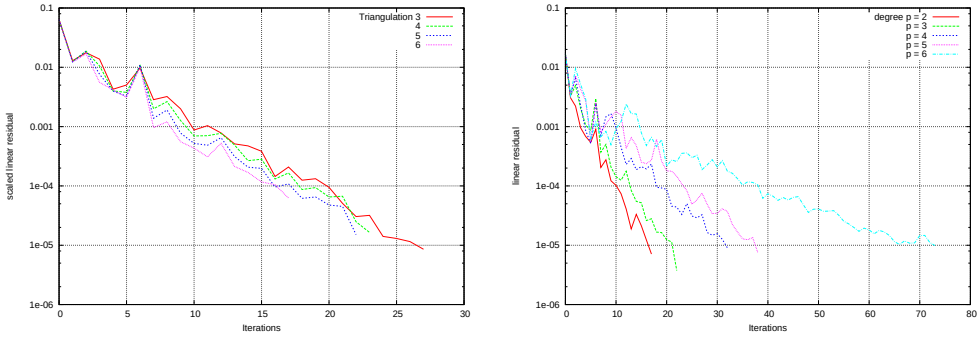

(a) Hierarchy of triangulations, $p = 3$. (b) Varying polynomial degree p on $\mathcal{T}^1_{h_5}$.

Figure 5. Solution process of PCG method for the Schur complement system arising from Problem 1. Diagonal preconditioning $\underline{\tilde{B}}_S^{-1}$, iterations vs. residual norm.

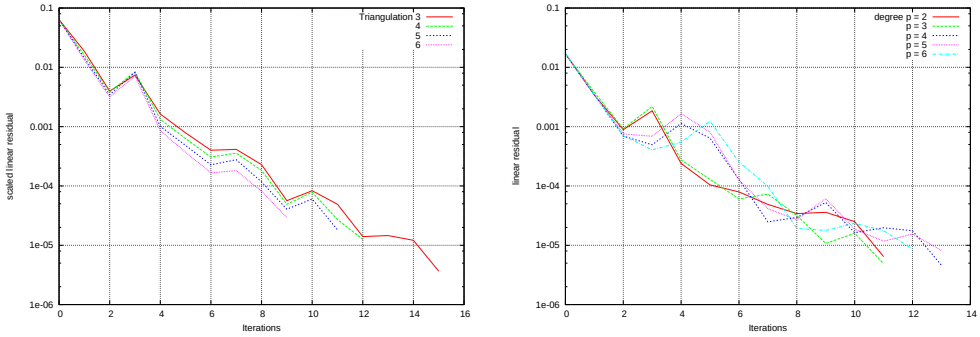

(a) Hierarchy of triangulations, $p = 3$. (b) Varying polynomial degree p on $\mathcal{T}^1_{h_5}$.

Figure 6. Solution process of PCG method for the Schur complement system arising from Problem 1. Block diagonal preconditioning $\underline{B}_S^{-1}$, iterations vs. residual norm.

irregular vertices. For these, the block diagonal preconditioner was modified in a way such that edges between elements of a different refinement level give rise to two edge blocks instead of a single one. The second part of Table 1 lists the approximate condition numbers for a hierarchy of uniformly refined grids. Shown in the first row, the condition number estimates for the unpreconditioned system grow rapidly with decreasing mesh size h. The estimates for the block preconditioner and the diagonal variant, listed in the second and third row, respectively, are again bounded. Compared to the diagonal edge variant, the block preconditioner still performs better.

5.2. *Advection-diffusion equation*

We examine the applicability of the presented preconditioner for a nonsymmetric system and consider the linear advection-diffusion problem (33) on the unit square domain $\Omega = [0, 1]^2$. Equation (33) is equipped with the Dirichlet boundary conditions except for $x_2 = 1$, where a Neumann boundary condition

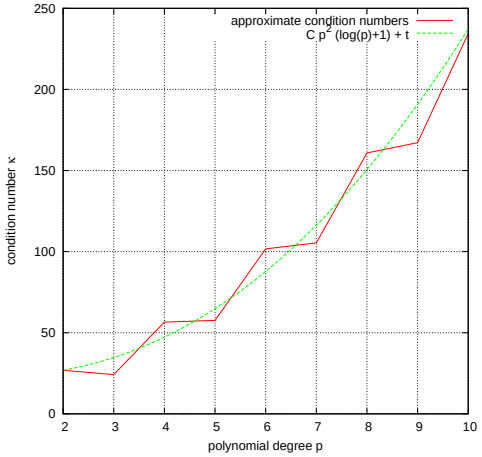

Figure 7. Approximated condition numbers of the PCG method for the Schur complement system arising from Problem 1 with block diagonal preconditioning $\underline{B}_S^{-1}$. Varying polynomial degree p on $\mathcal{T}_{h_5}^1$.

$$(\boldsymbol{a}\nabla u)\cdot\boldsymbol{n} = g_{\mathrm{N}} \equiv 0 \tag{34}$$

is applied. The data g_{D} on the Dirichlet boundary Γ_{D}, which contains the inflow part Γ_-, is given by

$$g_{\mathrm{D}} := \begin{cases} 5(x_1 - 0.2) & \text{for} \quad 0.2 < x_1 \leq 0.4, x_2 = 0, \\ 1 & \qquad\quad 0.4 < x_1 \leq 0.6, x_2 = 0, \\ 1 - 5(x_1 - 0.6) & \qquad\quad 0.6 < x_1 \leq 0.8, x_2 = 0, \\ 0 & \qquad\quad \text{elsewhere.} \end{cases}$$

For the hyperbolic part of equation (33) the standard upwind discretization with discontinuous finite elements is given by [15]

$$\begin{aligned} \sum_{\kappa\in\mathcal{T}_h}\int_\kappa (\boldsymbol{b}\cdot\nabla u)\, v \; d\boldsymbol{x} - \sum_{\kappa\in\mathcal{T}_h}\int_{\partial_-\kappa\setminus\Gamma} (\boldsymbol{b}\cdot\boldsymbol{n})[u]v^+ \; ds \\ - \sum_{\kappa\in\mathcal{T}_h}\int_{\partial_-\kappa\cap\Gamma} (\boldsymbol{b}\cdot\boldsymbol{n})u^+v^+ \; ds = -\sum_{\kappa\in\mathcal{T}_h}\int_{\partial_-\kappa\cap(\Gamma_-\cup\Gamma_{\mathrm{D}})} g_{\mathrm{D}}v^+(\boldsymbol{b}\cdot\boldsymbol{n}) \; ds, \end{aligned} \tag{35}$$

where $[v] := v_\kappa^+ - v_\kappa^-$ denotes the jump of the discrete solution function across the elemental inflow boundary $\partial_-\kappa = \{\boldsymbol{x}\in\partial\kappa \;:\; \boldsymbol{b}(\boldsymbol{x})\cdot\boldsymbol{n}(\boldsymbol{x}) < 0\}$.

The upwind discretization of the advection term leads to a nonsymmetric stiffness matrix $\underline{A}$, therefore the GMRES method is used for the iterative solution. Figure 8(a) shows an example solution of the discrete linear system for a value of $\epsilon = 10^{-3}$ on the triangulation $\mathcal{T}_h^3$. The preconditioning approach described in this paper works reasonably well for moderate values of ϵ. As illustrated in Figure 8(c), the behavior deteriorates for stronger perturbations of the elliptic term.

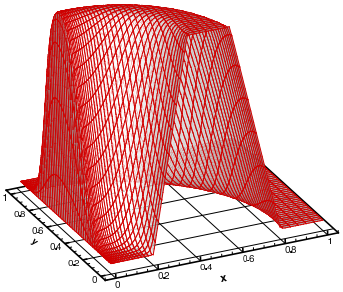

(a) Discrete solution, $\epsilon = 10^{-3}$

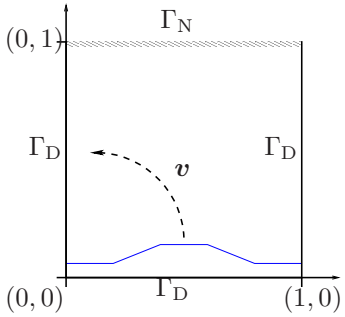

(b) Geometry

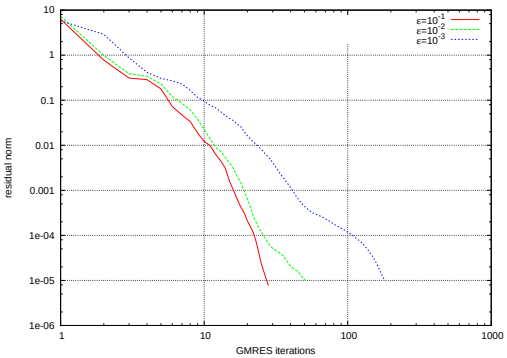

(c) Behavior of the block preconditioner for different values of ϵ

Figure 8. Numerical results for the advection-diffusion test Problem 2, polynomial degree $p = 2$.

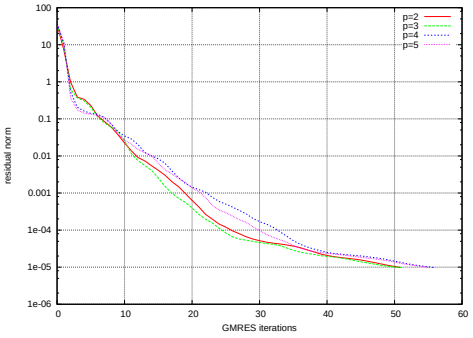

(a) Residual vs. iterations, $\epsilon = 10^{-2}$

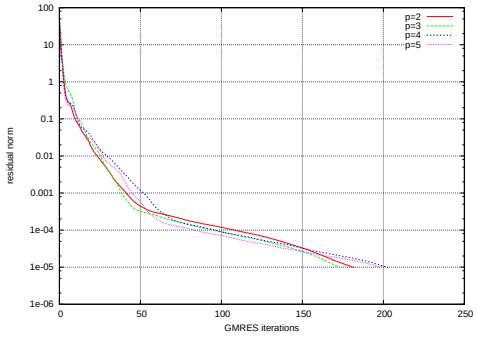

(b) Residual vs. iterations, $\epsilon = 10^{-3}$

Figure 9. p-Dependency of the iterative solution process for the advection-diffusion Problem 2.

6. Concluding remarks

The concept of low-order preconditioning for the finite element method has been successfully applied to the case of an interior penalty discontinuous Galerkin discretization. The numerical experiments support the results obtained from the analysis for elliptic problems and exhibit a convergence rate independent of the mesh refinement. The preconditioning method is amenable to parallelization and reduces the task of solving the linear equation system to an efficient solution of a global subproblem based on a discretization with bilinear elements.

Finally, we point out some restrictions of this class of preconditioners. The discussed iterative substructuring method requires a basis allowing a decomposition into external and internal degrees of freedom, see equation (8). The extension of the method from the two-dimensional case to three dimensions is nontrivial analogous to the conforming p-FEM [6]. Finally, the underlying theory was derived for the elliptic case. It should be clarified in how far the preconditioning technique can be generalized to indefinite, nonsymmetric problems, particularly to the convection dominated case.

Acknowledgements. Ralf Hartmann and Florian Prill acknowledge the partial financial support of both the President's Initiative and Networking Fund of the Helmholtz Association of German Research Centres and the European project ADIGMA [1]. The research of Mária Lukáčová was supported partially by the Deutsche Forschungsgemeinschaft under the grant LU 1470/1-1 and by the European Graduate School Differential Equations with Applications in Science and Engineering (DEASE), MEST-CT-2005-021122. The authors gratefully acknowledge these supports.

References

[1] ADIGMA. Adaptive higher-order variational methods for aerodynamic applications in industry. A specific targeted research project of the sixth European community framework programme, see http://www.dlr.de/as/desktopdefault.aspx/tabid-2035.

[2] D. N. Arnold, F. Brezzi, B. Cockburn, L. D. Marini, Unified analysis of discontinuous Galerkin methods for elliptic problems, SIAM J. Numer. Anal. 39 (5) (2002) 1749–1779.

[3] I. Babuška, A. Craig, J. Mandel, J. Pitkäranta, Efficient preconditioning for the p-version finite element method in two dimensions., SIAM J. Numer. Anal. 28 (3) (1991) 624–661.

[4] W. Bangerth, R. Hartmann, G. Kanschat, deal.ii – A general purpose object oriented finite element library, ACM Transactions on Mathematical Software 33 (4).

[5] W. Bangerth, R. Hartmann, G. Kanschat, `deal.II` Differential Equations Analysis Library, Technical Reference, http://www.dealii.org/, 6th ed., first edition 1999 (Sept 2007).

[6] M. A. Casarin, Schwarz preconditioners for spectral and mortar finite element methods with applications to incompressible fluids, Ph.D. thesis, New York University (1996).

[7] P. Castillo, Performance of Discontinuous Galerkin Methods for Elliptic PDEs, SIAM J. Sci. Comput. 24 (2) (2002) 524–547.
[8] P. G. Ciarlet, The finite element method for elliptic problems. 1st repr., vol. 4 of Studies in Mathematics and its Applications, North-Holland Publishing Company, Amsterdam, 1980.
[9] B. Cockburn, G. E. Karniadakis, C.-W. Shu, The development of discontinuous Galerkin methods., in: B. Cockburn, G. E. Karniadakis, C.-W. Shu (eds.), Discontinuous Galerkin methods. Theory, computation and applications. 1st international symposium on DGM, Newport, RI, USA, May 24-26, 1999 , vol. 11 of Lect. Notes Comput. Sci. Eng., Springer, Berlin, 2000, pp. 3–50.
[10] L. C. Evans, Partial differential equations., vol. 19 of Graduate Studies in Mathematics, American Mathematical Society (AMS), Providence, RI, 1998.
[11] E. H. Georgoulis, Discontinuous Galerkin methods on shape-regular and anisotropic meshes, Ph.D. thesis, University of Oxford (2003).
[12] C. Großmann, H.-G. Roos, Numerische Behandlung partieller Differentialgleichungen., Teubner Studienbücher Mathematik, Teubner, Wiesbaden, 2005.
[13] R. Hartmann, `PADGE`, Parallel Adaptive Discontinuous Galerkin Environment, Technical reference, DLR, Braunschweig, in preparation (2008).
[14] J. J. Heys, T. A. Manteuffel, S. F. McCormick, L. N. Olson, Algebraic multigrid for higher-order finite elements, J. Comput. Phys. 204 (2) (2005) 520–532.
[15] P. Houston, C. Schwab, E. Süli, Discontinuous *hp*-finite element methods for advection-diffusion-reaction problems., SIAM J. Numer. Anal. 39 (6) (2002) 2133–2163.
[16] N. Hu, X.-Z. Guo, I. N. Katz, Multi-*p* preconditioners., SIAM J. Sci. Comput. 18 (6) (1997) 1676–1697.
[17] N. Hu, I. N. Katz, Multi-*p* methods: Iterative algorithms for the *p*-version of the finite element analysis., SIAM J. Sci. Comput. 16 (6) (1995) 1308–1332.
[18] G. E. Karniadakis, S. J. Sherwin, Spectral/hp element methods for computational fluid dynamics. 2nd ed., Numerical Mathematics and Scientific Computation, Oxford University Press, Oxford, 2005.
[19] J. Kraus, S. Tomar, Multilevel preconditioning of elliptic problems discretized by a class of discontinuous Galerkin methods., Tech. rep., Johann Radon Institute for Computational and Applied Mathematics (RICAM) (2006).
[20] B. Q. Li, Discontinuous Finite Elements in Fluid Dynamics and Heat Transfer, Computational Fluid and Solid Mechanics, Springer, 2006.
[21] Y. Maday, R. Muñoz, Spectral element multigrid II: Theoretical justification., J. Sci. Comput. 3 (4) (1988) 323–353.
[22] J. Mandel, Iterative solvers by substructuring for the *p*-version finite element method., Comput. Methods Appl. Mech. Eng. 80 (1-3) (1990) 117–128.
[23] L. F. Pavarino, O. B. Widlund, A polylogarithmic bound for an iterative substructuring method for spectral elements in three dimensions, SIAM Journal on Numerical Analysis 33 (4) (1996) 1303–1335.
[24] S. Prudhomme, F. Pascal, J. T. Oden, A. Romkes, Review of A Priori Error Estimation for Discontinuous Galerkin Methods, Tech. rep., TICAM, Austin (2000).
[25] A. Quarteroni, A. Valli, Domain decomposition methods for partial differential equations., Numerical Mathematics and Scientific Computation, Clarendon Press, Oxford, 1999.

[26] W. Reed, T. Hill, Triangular Mesh Methods for the Neutron Transport Equation, Tech. rep., Los Alamos Scientific Laboratory (1973).
[27] E. M. Rønquist, A. T. Patera, Spectral element multigrid I: Formulation and numerical results., J. Sci. Comput. 2 (4) (1987) 389–406.
[28] Y. Saad, Iterative methods for sparse linear systems. 2nd ed., SIAM Society for Industrial and Applied Mathematics, Philadelphia, PA, 2003.
[29] C. Schwab, $p-$ and $hp-$finite element methods. Theory and applications in solid and fluid mechanics., Numerical Mathematics and Scientific Computation, Clarendon Press, Oxford, 1998.
[30] S. Sherwin, R. Kirby, J. Peiró, R. Taylor, O. Zienkiewicz, On 2D elliptic discontinuous Galerkin methods., Int. J. Numer. Methods Eng. 65 (5) (2006) 752–784.
[31] B. F. Smith, P. E. Bjørstad, W. D. Gropp, Domain decomposition. Parallel multilevel methods for elliptic partial differential equations., Cambridge University Press, Cambridge, 1996.
[32] P. Šolín, K. Segeth, I. Dolezel, Higher-order finite element methods., Studies in Advanced Mathematics, CRC Press, Boca Raton, 2004.
[33] A. Toselli, O. Widlund, Domain decomposition methods – algorithms and theory., vol. 34 of Springer Series in Computational Mathematics, Springer, Berlin, 2005.
[34] H. A. van der Vorst, Iterative Krylov methods for large linear systems., vol. 13 of Cambridge Monographs on Applied and Computational Mathematics, Cambridge University Press, Cambridge, 2003.